Enhancing the Mechanical Properties of Hydrogels with Vinyl-Functionalized Nanocrystalline Cellulose as a Green Crosslinker

Article *in* Nanotechnology · September 2023

DOI: 10.1088/1361-6528/acf93b

CITATIONS
0

READS
18

3 authors:

H B Muhammad Zukual Islam
Bangladesh University of Engineering and Technology
12 PUBLICATIONS **69** CITATIONS
SEE PROFILE

Suresh Babu Naidu Krishna
Durban University of Technology
76 PUBLICATIONS **1,113** CITATIONS
SEE PROFILE

Abu Bin Imran
Bangladesh University of Engineering and Technology
87 PUBLICATIONS **1,326** CITATIONS
SEE PROFILE

IOP Publishing Nanotechnology
Nanotechnology 34 (2023) 505706 (14pp) https://doi.org/10.1088/1361-6528/acf93b

Enhancing the mechanical properties of hydrogels with vinyl-functionalized nanocrystalline cellulose as a green crosslinker

Hasanul Banna Muhammad Zukaul Islam[1], **Suresh Babu Naidu Krishna**[2,3] **and Abu Bin Imran**[1,*]

[1] Department of Chemistry, Bangladesh University of Engineering and Technology, Dhaka 1000, Bangladesh
[2] Department of Biomedical and Clinical Technology, Durban University of Technology, Durban 4000, South Africa
[3] Institute of Water and Wastewater Technology, Durban University of Technology, Durban 4000, South Africa

E-mail: sureshk@dut.ac.za and abimran@chem.buet.ac.bd

Received 9 June 2023, revised 1 September 2023
Accepted for publication 12 September 2023
Published 4 October 2023

Abstract

Hydrogels have gained significant attention in scientific communities for their versatile applications, but several challenges need to be addressed to exploit their potential fully. Conventional hydrogels suffer from poor mechanical strength, limiting their use in many applications. Moreover, the crosslinking agents used to produce them are often toxic, carcinogenic, and not bio-friendly. This study presents a novel approach to overcome these limitations by using bio-friendly modified nanocrystalline cellulose as a crosslinker to prepare highly stretchable and tough thermosensitive hydrogels. The surface of nanocrystalline cellulose was modified with 3-methacryloxypropyltrimethoxysilane (MPTS) to obtain modified nanocrystalline cellulose (M-NCC) crosslinker and used during free radical polymerization of thermosensitive *N*-isopropyl acrylamide (NIPA) monomer to synthesize NIPA/M-NCC hydrogel. The resulting nanocomposite hydrogels exhibit superior mechanical, thermal, and temperature-responsive swelling properties compared to conventional hydrogels prepared with traditional bi-functional *N*, *N*′-methylene bis (acrylamide) (MBA) as a crosslinker. The elongation at break, tensile strength, and toughness of the NIPA/M-NCC hydrogels significantly increase and Young's modulus decrease than conventional hydrogel. The designed M-NCC crosslinker could be utilized to improve the mechanical strength of any polymeric elastomer or hydrogel systems produced through chain polymerization.

Keywords: hydrogel, biodegradable, stretchable, nanocomposite, crosslinker

(Some figures may appear in colour only in the online journal)

Introduction

Crosslinking provides chemical stability to polymeric materials, and when fabricating hydrogels, the addition of crosslinkers is necessary [1]. Both chemical and physical approaches have been employed to achieve polymeric networks [2]. Chemical methods include the reaction of complementary groups, polymer-polymer crosslinking, high-energy irradiation, and enzyme incorporation. Physical methods involve charge interactions, crystallization, and

* Author to whom any correspondence should be addressed.

stereo-complex formation. However, most conventionally used crosslinkers are toxic and not ideal for use [3–6]. They also exhibit poor water solubility and low biodegradation. Recently, there has been a growing interest in exploring biofriendly crosslinking agents as replacements for traditional crosslinkers [7, 8]. Researchers have developed crosslinking agents, such as silica, polyrotaxane, and clay, to develop polymeric hydrogels with improved mechanical properties [9–11]. These novel crosslinking agents can be utilized to produce polymeric materials with desirable characteristics. However, novel non-toxic crosslinkers need to be introduced to modulate release properties and achieve controlled biomedical applications of highly soluble and degradable polymers [12–17]. Considering the drawbacks associated with conventional crosslinkers, it is necessary to explore biofriendly novel crosslinking agents to formulate safe and efficient polymeric hydrogels. This study selected cellulose as a bio-friendly crosslinker alternative to conventional crosslinkers in polymer crosslinking processes.

Hydrogels are hydrophilic polymeric networks with a three-dimensional structure that can absorb and retain large amounts of water, saline, or physiological fluids while maintaining their swollen state under pressure [18]. Due to their high water content, porosity, and soft consistency, hydrogels closely resemble natural living tissue [19]. However, whether derived from natural or synthetic sources, they exhibit poor mechanical properties, which limit their industrial and biological applications [20–26]. The lack of effective energy dissipation mechanisms under stress and irregular distribution of crosslinking points contribute to the weak mechanical strength of hydrogels, leading to easy fracture initiation [27]. In recent years, significant efforts have been made to enhance the mechanical strength of hydrogels, resulting in the discovery of new hydrogel architectures with improved robustness. For instance, topological (TP) gels utilize figure-of-eight crosslinkers that can slide along polymer chains, allowing the gel to stretch significantly and exhibit a high swelling capacity [28]. Double-network (DN) hydrogels, created by incorporating a lightly crosslinked second network within a highly crosslinked first network, have been shown to possess exceptional strength and toughness [29]. Imran A B *et al* have reported a unique approach for making exceptionally flexible thermosensitive slide-ring hydrogels with good toughness by adding ionic groups into the polymer network and using polyrotaxane derivatives consisting of α-cyclodextrin and polyethylene glycol as crosslinkers [1, 30–32]. Nanocomposite (NC) hydrogels, formed by incorporating inorganic materials as crosslinking junctions, have demonstrated remarkable mechanical properties, thermal conductivity, biocompatibility, super hydrophilicity, and a higher swelling ratio [33]. The use of functionalized nanomaterials as additives or fillers in the preparation of NC hydrogels, such as clays, silica nanoparticles, carbon nanotubes, ferritin particles, and graphene oxide, has gained significant interest due to their easy fabrication, but they often lead to non-biodegradability and toxicity issues [34]. Biodegradable materials have become increasingly important in various practical applications, including super absorbents for personal hygiene products, water reservoirs in agriculture, body water retainers, stomach bulking agents, scaffolds for regenerative medicine, controlled drug delivery systems, wound dressings, and other biomedical applications [35–37]. Natural polymers like starch, cellulose, and nanocellulosic materials, such as cellulose nanocrystals, cellulose nanofibers, and bacterial nanocellulose, have attracted attention as promising biodegradable material options for NC hydrogels [38, 39].

Polymeric nanocomposite materials, including hydrogels, elastomers, and films, have been developed using reinforcing agents or fillers such as cellulose nanofibrils (CNF), nanocrystalline cellulose, starch nanoparticles, and nanoclay [21, 40–42]. Various crosslinking agents and catalysts have been investigated to produce cellulose-derived hydrogels, with common examples including epichlorohydrin, aldehydes, urea derivatives, carbodiimides, and carboxylic acids [43]. Functionalized nanocrystalline cellulose (NCC) has been successfully incorporated into hydrogels to enhance their mechanical properties [44]. Chemical incorporation of NCC into polymer hydrogel networks through the formation of covalent bonds is more beneficial than physical incorporation [45]. Surface modification of NCC is an essential step to introduce specific functional groups, achieved through direct chemical modification, physical interaction, or adsorption to the NCC's surface. Researchers have developed nanocomposite hydrogels with rod-like cellulose nanocrystals as reinforcing fillers into polymeric hydrogels, resulting in improved mechanical strength and flexibility [46]. Other studies have demonstrated structurally and physically anisotropic hydrogels based on hydrazone crosslinked poly(oligoethylene glycol methacrylate) (POEGMA) and aldehyde-functionalized NCC, which show great structural integrity and mechanical properties, making them suitable for tissue engineering [47]. Injectable polysaccharide hydrogels based on cellulose acetoacetate (CAA), hydroxypropyl chitosan (HPCS), and amino-modified NCC (NCC-NH_2) have also been developed, exhibiting pH-responsive and self-healing properties, as well as good biocompatibility for biomedical applications [48]. A novel NC hydrogel with antibacterial and antioxidant properties was developed by combining sodium carboxymethylated starch (CMS), a natural polymer, with CuO nanoparticles for wound healing applications [49]. Hydrogel nanocomposites based on CMS/PVA containing AgNPs were developed, where CMS and PVA were utilized as green reducing agents in the production of AgNPs. The properties of CMS/PVA hydrogel nanocomposites, including swelling degree, rheology, silver ion release kinetics, antibacterial activity, and toxicity, were investigated by examining the influence of $AgNO_3$ concentration on human fibroblasts [50]. Hydrophobically modified clay has been chosen as an inorganic additive in the hydrogel matrix because of its stronger interactions with the polymer chains, which can enhance the intrinsic qualities of the hydrogel. Polyethyleneimine (PEI) was selected as the crosslinking agent, and hydrogels, namely partially hydrolyzed polyacrylamide (HPAM) /PEI conventional hydrogels, HPAM/PEI/Bent, and HPAM/PEI/Orgbent, were produced using

Table 1. Preparation recipe of NIPA/M-NCC nanocomposite hydrogels with varying crosslinker and monomer concentrations.

Sample name	NIPA (M)	M-NCC (wt%)	KPS (mM)	TEMED (μl)
NIPA (2)/M-NCC 0.10 wt%	2.00	0.10	2.96	20
NIPA (2)//M-NCC 0.50 wt%	2.00	0.50	2.96	20
NIPA (2)//M-NCC 0.75 wt%	2.00	0.75	2.96	20
NIPA (2)//M-NCC 1.0 wt%	2.00	1.00	2.96	20
NIPA (3)//M-NCC 0.25 wt%	3.00	0.25	2.96	20
NIPA (3)//M-NCC 0.50 wt%	3.00	0.50	2.96	20
NIPA (3)//M-NCC 0.75 wt%	3.00	0.75	2.96	20
NIPA (3)//M-NCC 1.0 wt%	3.00	1.00	2.96	20
NIPA (4)//M-NCC 0.75 wt%	4.00	0.75	2.96	20

varying concentrations of clay [51]. However, a significant issue faced by these fabricated materials is their inadequate mechanical properties resulting from the absence of strong covalent interactions of polymer chains with natural fillers or crosslinkers in most cases. To address this challenge, the focus of this research is to employ vinyl modified nanocrystalline cellulose as a multifunctional and bio-friendly crosslinker. Through free radical polymerization, the crosslinker will be combined with diverse monomers during polymerization to fabricate a polymeric nanocomposite hydrogel that is highly flexible and mechanically robust.

Experimental

Materials

Microcrystalline cellulose (MCC) from Qualikems Fine Chem, 3-Methacryloxypropyltrimethoxysilane (MPTS), *N,N,N′,N′*-Tetramethyl ethylenediamine (TEMED), and acetic acid from Sigma Aldrich, *N*-isopropyl acrylamide (NIPA) from K J Chemical Corporation in Japan, potassium persulfate (KPS) and ethanol from Merck Germany, sulfuric acid from RCI Lab Scan were purchased and used as received. Aqueous solutions for all experiments were prepared using deionized (DI) water unless stated otherwise.

Synthesis of NCC form MCC

The optimization of NCC preparation was performed by varying acid concentration, MCC to acid ratio, hydrolysis time, hydrolysis temperature, and ultrasonic time and power [52]. A 200 ml 64% (w/w) H_2SO_4 (MCC-to-acid weight ratio of 1 to 20) was adjusted to the desired temperature. Upon reaching the specified temperature, H_2SO_4 was added to the cellulose in the round bottom flask. The resulting mixture was hydrolyzed at 60 °C for 90 min with continuous stirring. To avoid overheating, ultrasonication was applied every 30 min while simultaneously cooling the reaction using an ice bath. The suspension was diluted tenfold to stop the reaction and left to settle for several hours until distinct layers formed. The transparent top layer was carefully decanted, and the suspensions were subjected to repeated rinsing with distilled water until no layering was observed. The suspension was then transferred to centrifuge tubes, and centrifugation was performed at 4000 rpm for 10 min to remove excess acid and water-soluble particles. At a pH of approximately 4, the fine cellulose particles dispersion in the water was observed. The turbid supernatant containing polydisperse cellulose particles was collected, and the NCC suspension was further separated by centrifugation at 4000 rpm for 10–15 min. Following this, the suspension was rinsed with deionized water. The technique was repeated four to five times for each sample to lower the acid concentration. Subsequently, the suspension underwent dialysis against deionized water in regenerated cellulose dialysis tubes with a molecular weight cutoff of 12 000–14 000 Dalton. The dialysis process was continued for several days until the pH of the water remained constant. The purified NCC suspension was then stored at 5 °C in a refrigerator. A fraction of the dialyzed NCC was freeze-dried to obtain a powdered sample for further analysis.

Modification of NCC by MPTS

The silanization of NCC was performed using MPTS. A 10% (w/w) MPTS solution was prepared in an ethanol-water mixture (9:1 vol. percent) for hydrolysis. The pH of the solution was adjusted to 3–4 by adding a 0.1 mol L^{-1} acetic acid solution. Subsequently, the hydrophilic NCC was added to the solution. The resulting mixture was heated in an oil bath at a temperature range of 60 °C–70 °C while being agitated at 500 rpm for 30 min. After the completion of the reaction, centrifugation was employed to separate the particles. The silanized NCC product was then immersed in deionized water for 24 h to remove any residual reactants. The product was rinsed multiple times with deionized water to remove the effects of physical adsorption. The silanized NCC was subsequently dried at room temperature for two days to remove excess moisture. The dried product was further heated at 80 °C for an additional 4 h.

Synthesis of NIPA/M-NCC nanocomposite hydrogel

The NIPA/M-NCC hydrogel was prepared by conducting free radical polymerization of NIPA in the presence of the KPS initiator [45]. The M-NCC crosslinker was initially dispersed in distilled water to ensure uniform distribution. Subsequently, a fixed molar concentration of NIPA monomer was dissolved in the solution and subjected to sonication for a minute. Varying amounts of M-NCC was then added to the NIPA solution, with the specific percentages detailed in

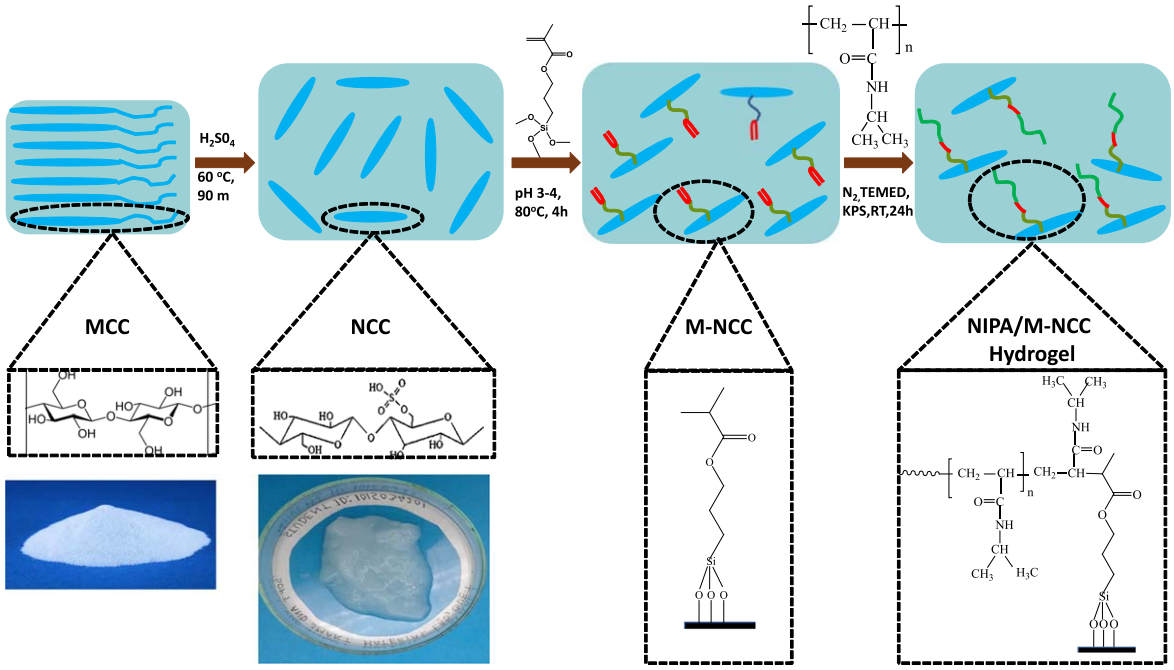

Scheme 1. Schematic representation of the preparation of NCC, M-NCC, and NIPA/M-NCC nanocomposite hydrogel.

table 1. The solution was then bubbled with N_2 gas to make the solution free from oxygen. A small amount of TEMED was mixed in the solution, which worked as an accelerator for free radical polymerization reaction. 2.96 mM KPS initiator solution was bubbled in another container with N_2 gas. Then two solutions were mixed immediately in an ice bath and transferred to a glass cell separated with a teflon spacer of desired shape and size. A glass test tube is used to synthesize cylindrical hydrogels. The polymerization was carried out at room temperature for 24 h. Hydrogels were carefully removed from glass cells or test tubes after polymerization. For further characterization, the slab hydrogels were cut into pieces of roughly 12 mm length and 10 mm width obtained in rectangular shapes.

Characterizations

Morphological study. The particle size of NCC, M-NCC, and the surface morphology of the hydrogels were examined using a field emission scanning electron microscope (FE-SEM: JEOL, JSM, 7600 F). Prior to analysis, the samples were coated with gold using a fine auto coater (JEOL JFC-1600, Japan). An energy-dispersive x-ray spectrometer (EDX) coupled with the FE-SEM was used to determine the elemental identification and quantitative compositional information of the samples.

Structural analysis. A Fourier transform infrared (FT-IR) spectrometer (Shimadzu, Japan) was used to confirm the successful modification of NCC and its interactions within the polymer networks. The samples were freeze-dried, ground, and properly mixed with KBr (Sigma Aldrich, Germany).

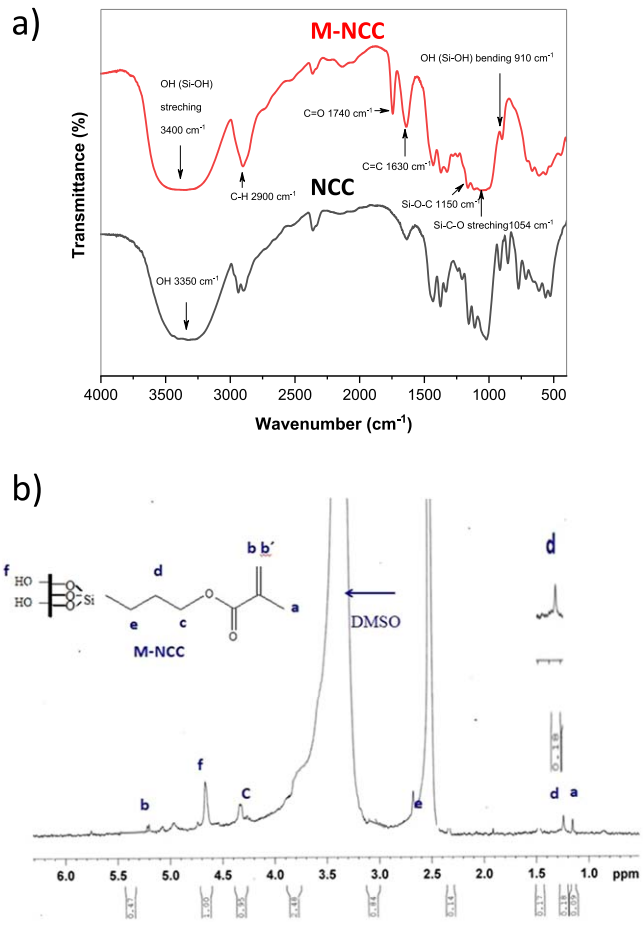

Figure 1. (a) FT-IR spectra of NCC and M-NCC (b) ^{1}H-NMR spectra of M-NCC.

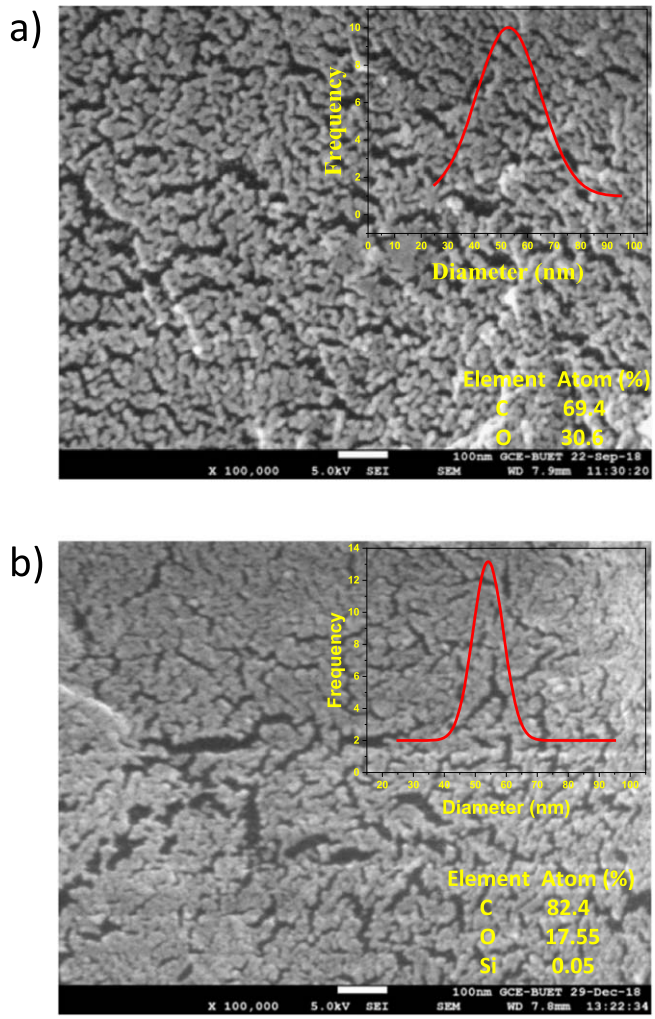

Figure 2. (a) FESEM images of as-prepared NCC (inset of figure 2(a) denotes particle size distribution curve of NCC) (b) FESEM images of as-prepared M-NCC (inset of figure 2(b) denotes particle size distribution curve of M-NCC).

Sample pellets were prepared using a manual hydraulic press, and spectra was collected in the 400–4000 cm^{-1} frequency range.

A Bruker BPX- 400 spectrometer running at 400 MHz was used to record the ^{1}H-NMR spectra. DMSO was used as a solvent and the internal standard was tetramethylsilane (TMS). All chemical shifts (δ) and coupling constants (J) were measured in ppm and Hz. Chemical shifts were measured with respect to the peaks of TMS and d-DMSO.

Mechanical analysis. Rectangular-shaped samples (10.0 ± 0.1 mm in diameter and 12.0 ± 0.1 mm in length) were subjected to tensile stress–strain measurements using a universal testing machine (UTM, Test Resources, Model 100-P-250-12) at room temperature. The crosshead speed was set to 10.0 mm per minute. The tensile stress (σ) of the hydrogel was determined based on force per area, while the strain (%) was calculated by dividing the change in length (Δl) by the original length (l). The slope of the stress–strain curves during the initial 10% deformation was used to calculate Young's modulus. The area under the stress–strain curves was also utilized to determine the toughness of each sample. Tensile strength was measured at the highest stress point, and elongation at break (%) was determined at the maximum strain tolerance before rupture. The compressive tests of hydrogels were also carried out on a UTM at room temperature. The cylindrical hydrogel samples having a diameter of 10 mm and a thickness ranging from 5 to 8 mm were used for compressive analysis. To ensure reproducibility, each specimen was tested at least three times.

Thermal analysis. The thermal behavior of the samples was evaluated using a differential scanning calorimeter (DSC) and Thermo Gravimetric Analysis (TGA) (STA-449 F3, Jupiter, NETZSCH) under N_2 atmospheres at a heating rate of 5 °C min^{-1}. Samples weighing 5–10 mg were heated from room temperature to 900 °C, and the weight loss of the samples was measured as a function of temperature. During the measurements, air was purged at a rate of 20 ml min^{-1}.

Swelling behaviors of hydrogels. The swelling ratios of NIPA/M-NCC nanocomposite hydrogels were measured in the temperature range of 10 °C–60 °C. After freeze-drying, hydrogel samples were immersed and equilibrated in distilled water at a specific temperature controlled by a water circulation bath and the temperature-dependent swelling ratio of the sample was measured. The swelling ratios of the samples were calculated using the equation, $SR = \frac{W_s - W_d}{W_d}$, where SR stands for swelling ratio, W_s for swollen hydrogel mass, and W_d for dry hydrogel mass.

Results and discussion

To introduce vinyl groups onto the surface, the hydroxyl groups of NCC are functionalized with MPTS. Scheme 1 illustrates our approach for preparing the crosslinker M-NCC from NCC. The FT-IR spectra of NCC and M-NCC are shown in figure 1(a), providing substantial support for the successful functional groups incorporation. The Si–OH groups of the hydrolyzed MPTS were first formed on the NCC surface. Water was removed after 4 h of thermal treatment at 80 °C, and covalent bonds were established between NCC and MPTS, resulting in vinyl functional M-NCC via silane exchange. The typical absorption peaks of the Si–O–C bonds in the 1150 cm^{-1} and 1270 cm^{-1} range are observed [53]. Additionally, the 1630 cm^{-1} and 1740 cm^{-1} peaks are assigned to the stretching vibrations of C=C and C=O, respectively. The FT-IR spectra also showed the presence of hydrogen-bonded −OH stretching at 3600–3200 cm^{-1}, C-H stretching at 2900 cm^{-1}, and Si–OH bending at 910 cm^{-1}. These observations support the successful modification process and the presence of specific functional groups in the NCC and M-NCC samples.

Figure 1(b) displays the chemical shifts observed in the NMR spectrum of the silanes involved in the surface chemical modification of NCC. The 5–5.5 ppm range signals are attributed to the vinyl groups, with a singlet at 1H for C–b and

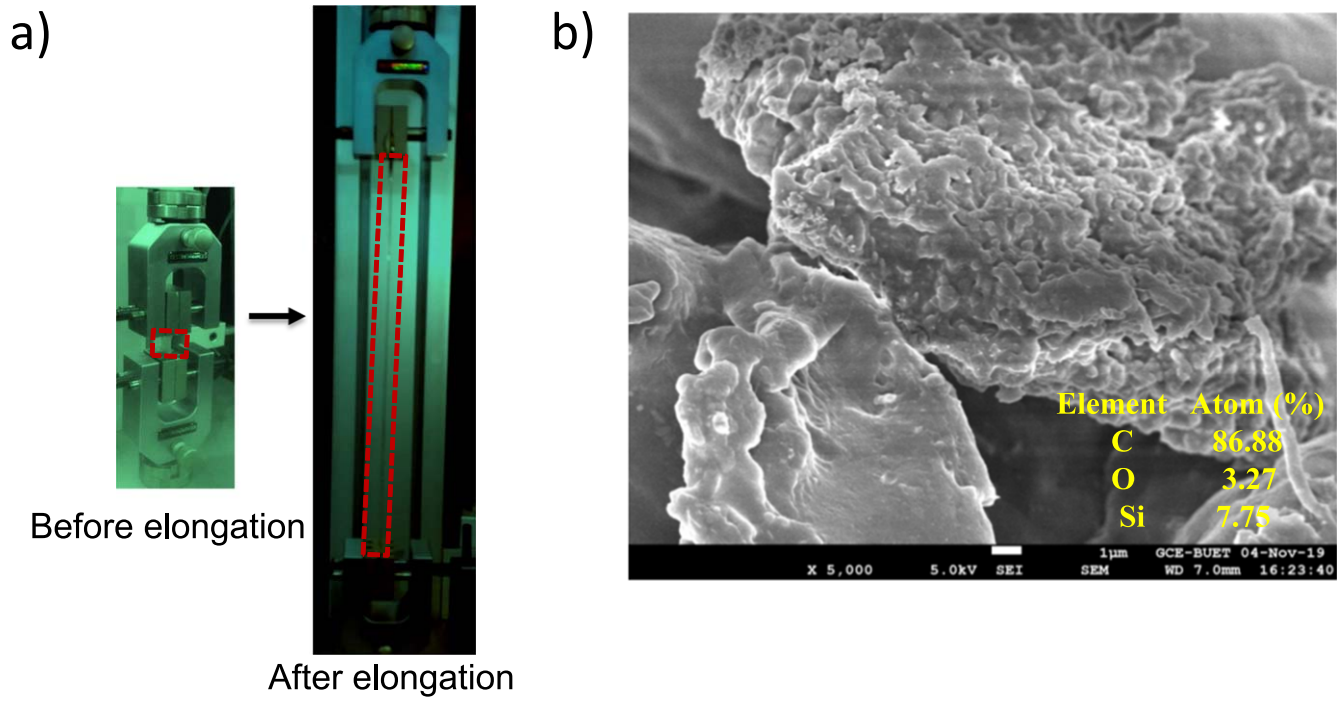

Figure 3. (a) Photograph of highly transparent as synthesized NIPA/M-NCC hydrogel before and after elongation (b) FE-SEM image of NIPA/M-NCC 0.5 wt% nanocomposite hydrogel.

another at ^{1}H for C–b′ positions, respectively. The peaks at δ 1.0–1.5 ppm (^{1}H singlet for –CH_3), δ 4.0–4.5 ppm (^{1}H triplet for –CH_2–), δ 1.0–1.5 ppm (^{1}H pentet for –CH_2–), δ 2.5–3.0 ppm (^{1}H triplet for –CH_2–), δ 4.5–5.0 ppm (^{1}H singlet for −OH). These chemical shifts indicate that the silane coupling agent has effectively modified the NCC to obtain M-NCC crosslinker.

The FESEM image of the synthesized NCC, depicted in figure 2(a), exhibited a uniform size and shape. Even after the modification with MPTS, the FESEM micrograph of M-NCC, shown in figure 2(b), displayed a similar morphology. This observation suggests that no substantial changes in the shape of the particles occurred during the modification process, indicating that the MPTS modification did not significantly alter the overall shape of the particles.

Inset of figures 2(a) and (b) show size distribution histograms for both NCC and M-NCC samples. The particle size distribution for both NCC and M-NCC appeared narrow. However, the modification process using MPTS led to a slight increase in the average particle size, as indicated by the Gaussian distribution. The average particle size changed from 53 ± 10 nm for NCC to 55 ± 10 nm for M-NCC. EDX analysis confirmed the successful modification of MPTS on NCC. The atomic percentages of carbon, oxygen, and silicon in M-NCC are 82.4%, 17.55%, and 0.05%, respectively, thereby validating the introduction of MPTS onto the surface.

The synthesis of NIPA/M-NCC nanocomposite hydrogels involved using a free radical polymerization reaction, where poly (NIPA) chains were crosslinked with M-NCC. The porosity of the NIPA/M-NCC hydrogel was examined through FESEM analysis of the freeze-dried NIPA/M-NCC 0.5 wt% hydrogel. During the freeze-drying process, water molecules were removed, forming sponge-like interconnecting micropores [54], as depicted in figure 3. Most of the pore sizes were smaller than 1 μm and evenly distributed. Scheme 1 illustrates a schematic diagram of the stepwise synthesis of the NIPA/M-NCC nanocomposite hydrogel.

The SEM image displayed a polymeric layer on M-NCC, which could be attributed to a significant amount of 2D surface crosslinking of M-NCC with monomer. The available vinyl groups on M-NCC facilitated strong covalent interactions with the poly (NIPA) chains during polymerization, leading to enhanced mechanical properties. No apparent aggregation in the SEM images, suggesting that crosslinking achieved through the combination of M-NCC and poly (NIPA) was maintained homogeneity. To understand the influence of M-NCC on the mechanical properties of NIPA/M-NCC hydrogels, various parameters such as crosslinker type, concentration, and water content were tested. Under applied external stress, the prepared NIPA/M-NCC hydrogels exhibit remarkable tensile and compressive properties. The NIPA (2)/M-NCC 0.75 wt% hydrogel is highly stretchable and can be elongated more than 31 times from its initial length. It shows high elongation at break, tensile strength, and toughness. On the other hand, conventional NIPA (2)/BIS 0.75 wt% hydrogel prepared using 0.75 wt% MBA crosslinker showed poor mechanical properties (figure 4). The elongation at break, tensile strength, and toughness (figure 5) of NIPA (2)/M-NCC hydrogels with varying crosslinker concentrations are increased with increasing crosslinker amount up to a certain level. However, the scenario differs at high concentrations due to inhomogeneous crosslinker dispersion, as shown in figure 5. The NIPA (2)/M-NCC

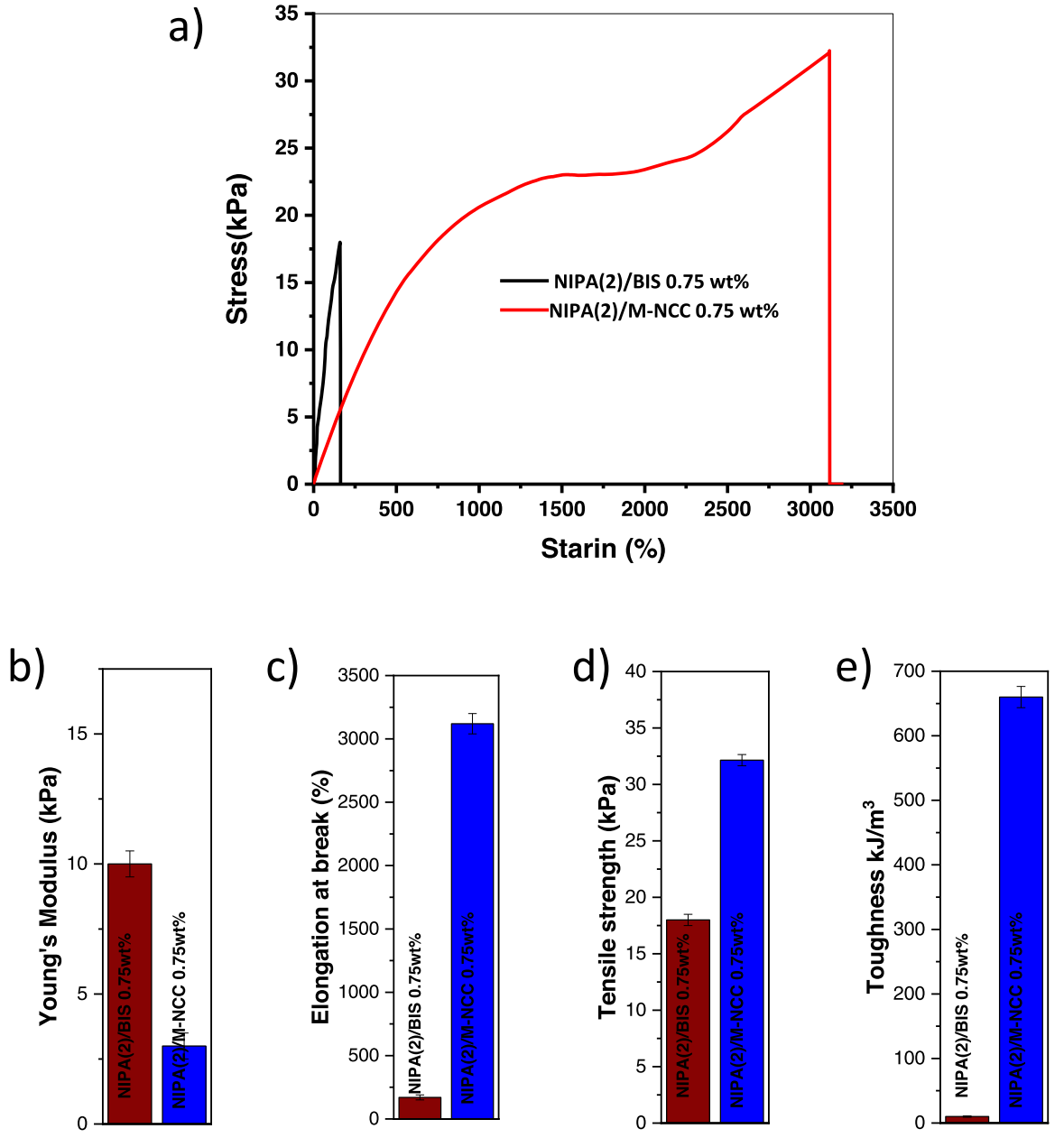

Figure 4. A comparative mechanical analysis of MBA based conventional NIPA (2)/BIS 0.75 wt% hydrogel (represented by the dark red line) and an M-NCC based NIPA (2)/M-NCC 0.75 wt% nanocomposite hydrogel (represented by the blue line) (a) uniaxial stress–strain curves (b) Young's modulus, (c) elongation at break, (d) tensile strength, and (e) toughness.

0.75 wt% nanocomposite hydrogel exhibits the most significant improvements elongation at break, tensile strength, and toughness compared to other crosslinker content variation. The 0.75% M-NCC may be dispersed well and form uniform crosslinking density with poly (NIPA) chains, contributing to the improved mechanical properties of the NIPA (2)/M-NCC 0.75 wt% hydrogel.

The NIPA (2)/M-NCC 0.75 wt% hydrogel also exhibits strain-hardening behavior at high elongation. This strain hardening phenomenon can be attributed due to the limited movement of poly (NIPA) chains after the expansion of polymer networks with sparsely and homogeneously distributed M-NCC with poly (NIPA) chains, as depicted in figure 5 (blue curve).

The tensile strength, Young's modulus, elongation at break and toughness for MBA crosslinker based conventional hydrogel are very low compared to NIPA (3)/M-NCC hydrogels.

The results of tensile tests conducted on other NIPA (3)-M-NCC and NIPA (4)-M-NCC hydrogels with varying crosslinker concentrations were observed to be similar to the NIPA (2)-M-NCC hydrogels. The elongation at break, tensile strength, and toughness increase with crosslinker concentration up to a certain threshold. However, at very high concentrations, these properties begin to decrease due to the inhomogeneous distribution of the crosslinker within the polymer networks. In contrast, Young's modulus generally

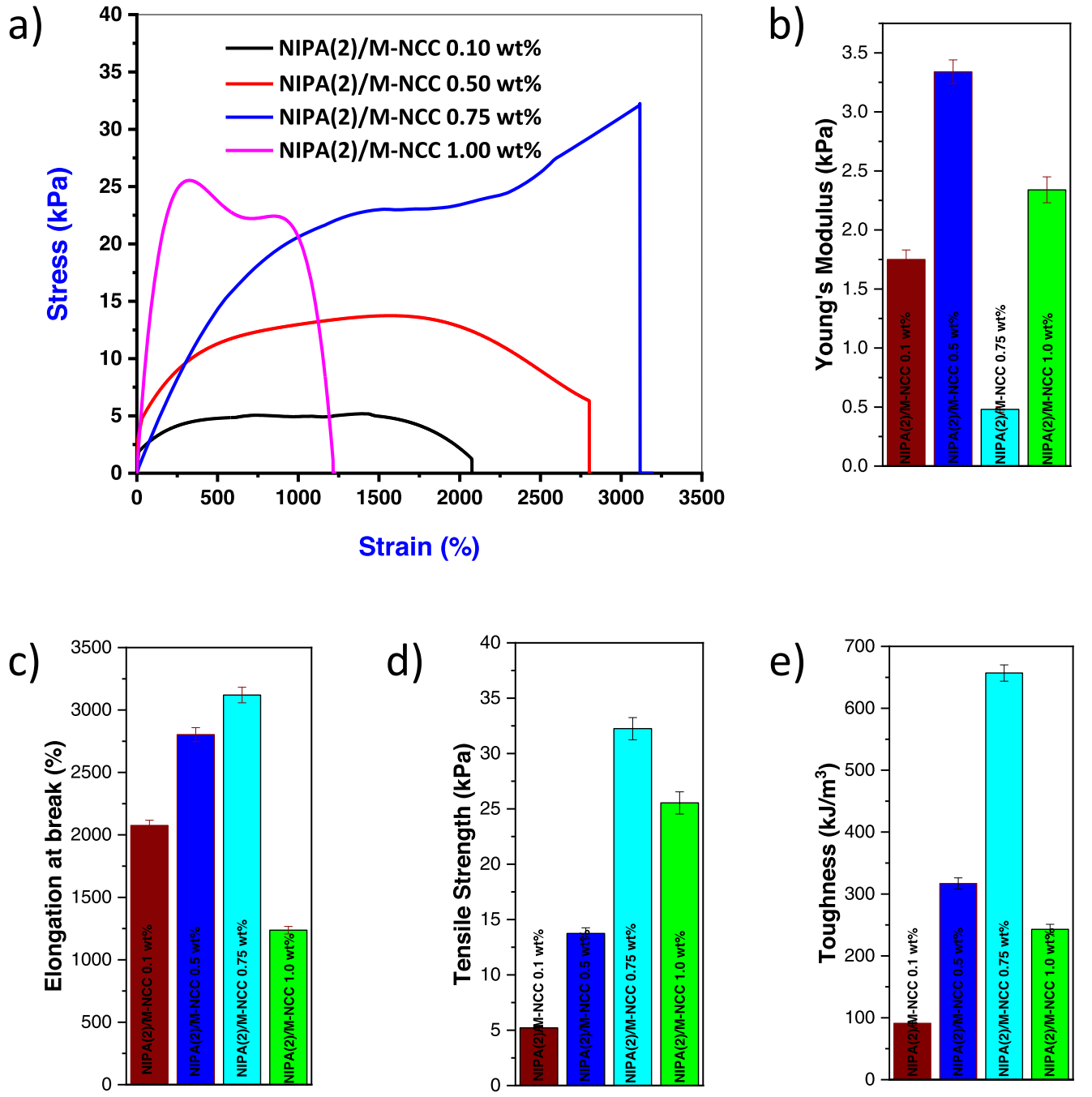

Figure 5. Tensile properties of NIPA(2)/M-NCC hydrogels with varying amounts of M-NCC crosslinker (a) uniaxial stress–strain curves, (b) Young's modulus, (c) elongation at break, (d) tensile strength, and (d) toughness.

increases with the rise in crosslinker concentration, except for the NIPA (3)/M-NCC 0.25 wt% nanocomposite hydrogel. The Young's modulus NIPA (2)/M-NCC hydrogel is lower than MBA crosslinker-based NIPA (2)/BIS hydrogel. This behavior suggests a soft and flexible nature of the polymer networks in NIPA (2)/M-NCC hydrogels.

The monomer concentration was found to impact the mechanical properties of NIPA/M-NCC nanocomposite hydrogels. Figure 6 shows that the NIPA (4)/M-NCC 0.75 wt% nanocomposite hydrogel exhibits the highest tensile strength but the lowest toughness. This can be attributed to the rigid behavior associated with a higher monomer ratio. NIPA (2)/M-NCC 0.75 wt% nanocomposite hydrogel has the greatest elongation and toughness. The softness and flexibility of the poly (NIPA) chains and uniformly dispersed cross-linker, allow for energy dissipation during deformation, contributing to enhanced elongation and toughness properties. The Young's modulus of NIPA (2)/M-NCC hydrogel increases with increasing monomer amount. The dramatic increase in Young's modulus with monomer concentration is

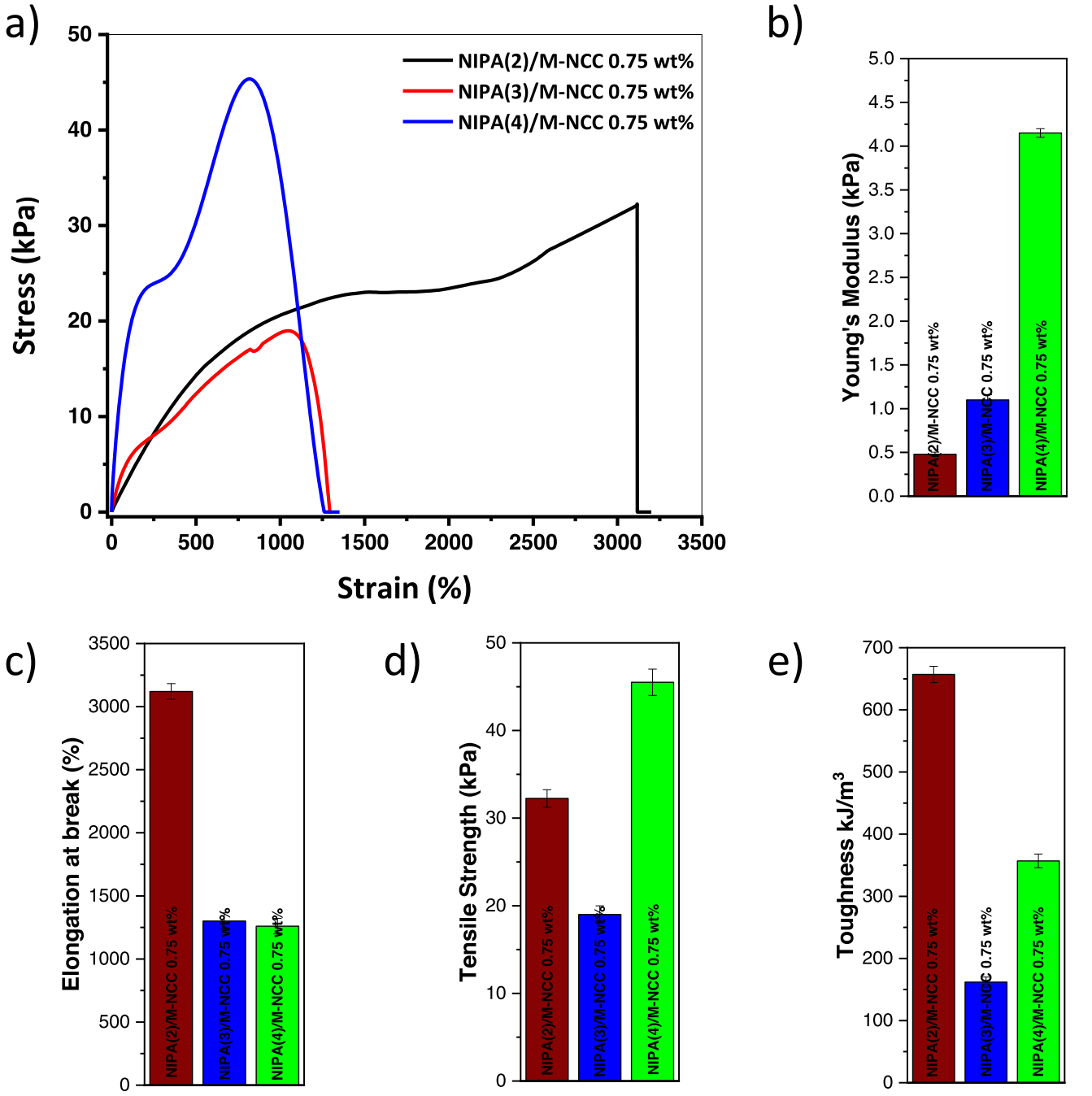

Figure 6. Tensile properties of NIPA (2)/M-NCC hydrogels with varying amounts of monomer concentration (a) uniaxial stress–strain curves, (b) Young's modulus, (c) elongation at break, (d) tensile strength, and (d) toughness.

due to the increased interaction between the monomer and the M-NCC crosslinker. As the monomer concentration rises, the entanglement of the polymer chains and the contact between the poly (NIPA) and M-NCC crosslinker also increase. These interactions contribute to the rigidity and stiffness of the NIPA/M-NCC hydrogel, significantly increasing Young's modulus.

Figure 7(a) represents the uniaxial stress–strain curves of NIPA (3)/M-NCC hydrogels with varying crosslinker amounts. All hydrogel samples maintained their shape and didn't rupture during 70% strain. The NIPA (3)/M-NCC 0.75% hydrogel exhibits the highest stress response under 70% strain. The Young's, modulus, compressive strength, and toughness of NIPA (3)/M-NCC 0.75 wt% are highest compared to others. Use of M-NCC by more than 0.75% starts to decrease the compressive properties in all aspects. The distribution of M-NCC may not be homogeneous and some aggregation of M-NCC may occur before forming polymer networks. As a result, the compressive properties significantly varied for NIPA (3)/M-NCC 1.0 wt% hydrogel.

The enhancement in compressive strength of NIPA (3)/M-NCC hydrogel is observed to be directly influenced by the

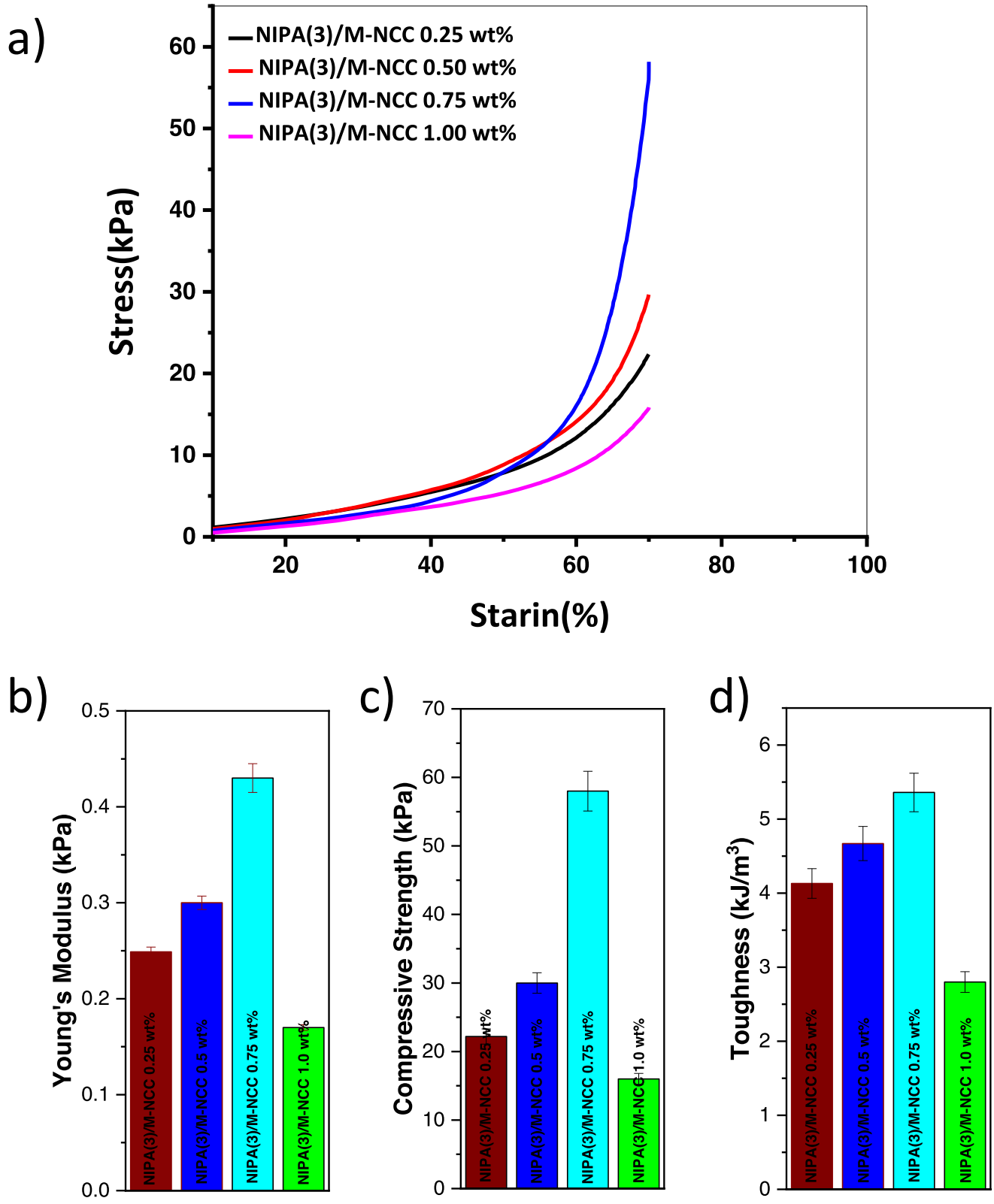

Figure 7. Compressive properties of NIPA (3)/M-NCC hydrogels with varying amounts of M-NCC crosslinker (a) uniaxial stress–strain curves, (b)Young's modulus, (c) compressive strength, and (d) toughness.

crosslinker concentration. As the extent of compression increases, the network gradually becomes denser, leading to decreased flexibility of the gels. A reduction in breaking strains as the crosslinker concentration increases are attributable to the increased covalent bonding density. Using M-NCC as a crosslinker notably enhances the compressive strength of NIPA/M-NCC nanocomposite hydrogels. The strong interaction between the NIPA polymer chain and the

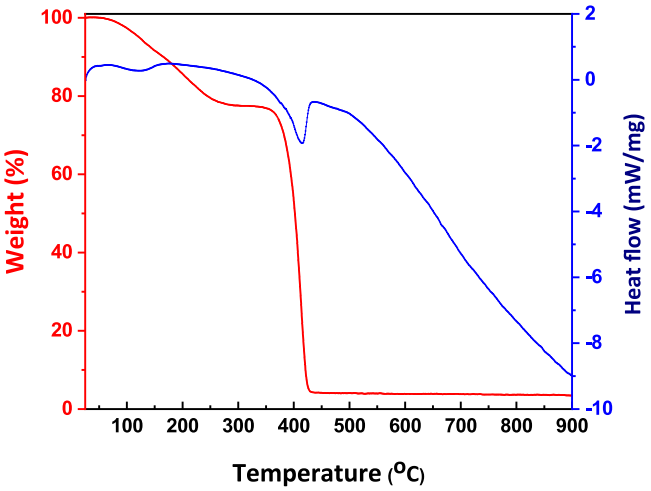

Figure 8. TGA and DSC curves of NIPA/M-NCC nanocomposite hydrogel.

M-NCC crosslinker and favorable uniform distribution of M-NCC results in higher strength for NIPA/M-NCC nanocomposite hydrogels. Consequently, an increase in crosslinker concentration in the formulation elevates the hydrogel fraction, thereby boosting compression strength, toughness, and Young's modulus up to a certain point. However, these properties begin to decline at very high M-NCC crosslinker concentrations.

Thermal TGA-DSC analyses were conducted from room temperature to 900 °C with a heating rate of 5 °C per minute under a N_2 environment. Most of the weight loss below 200 °C in the NIPA (2)/M-NCC 0.75 wt% hydrogel can be attributed to the loss of water [55, 56]. When the pure poly (NIPA) hydrogel is decomposed in the temperature range of 330 °C–580 °C, it experiences a significant mass loss of 94.9%. The addition of M-NCC at a concentration of 0.5 wt% reduced thermal stability which is attributed to the increased surface area of M-NCC, providing additional sites for rapid degradation (figure 8). The initial 14% mass loss below 200 °C is due to water loss from the polymer network. The second step involves decomposition at temperatures between 330 °C and 420 °C, leading to a 96% mass loss. This indicates lower thermal stability than pure poly (NIPA) and suggests the better degradability of the NIPA/M-NCC nanocomposite hydrogel. The DSC curve exhibits an endothermic peak at approximately 415 °C. The glass transition temperature (Tg) at 128 °C is hardly observable on the DSC curve, while the reported Tg for pure NIPA is 130 °C [57].

Figure 9(a) illustrates the temperature-dependent swelling behavior of the NIPA (2)/M-NCC nanocomposite hydrogel with varying crosslinker amounts. Water absorption behavior at different temperatures in the range of 20 °C–60 °C was used to track changes in the weight of hydrogels with temperature change. In all circumstances, the equilibrium swelling ratio decreases as the temperature rises. The swelling ratio of a NIPA (2)/M-NCC hydrogel with crosslinking undergoes a significant change between 30 °C and 40 °C due to increased hydrophobic forces at higher temperatures, leading to phase separation of the hydrogel [58, 59]. The hydrogel swells in an aqueous solution below the LCST of NIPA, approximately 31 °C, while dramatically shrinks above this temperature. Slight temperature variations cause reversible breaking and formation of hydrogen bonds between the N–H or C=O group of NIPA and the surrounding water molecules. The hydration force decreases as the temperature rises, and the increased hydrophobic force of poly (NIPA) assists in forming a globular configuration. As a result, phase separation of hydrogel occurs at a certain temperature around LCST temperature of NIPA. Furthermore, the swelling ratio of NIPA (2)/M-NCC nanocomposite hydrogels decreases with increasing crosslinker content ranging from 0.025% to 1.00%. The swelling behavior of NIPA (2)/M-NCC hydrogels is primarily influenced by the M-NCC content, with higher M-NCC leading to lower swelling ratios. The presence of crosslinker hinders the swelling of the hydrogel, as the movement of polymer chains is restricted due to increased crosslinking density. The swelling capacity of the NIPA/M-NCC nanocomposite hydrogels decreases with increasing crosslinker amount. Figure 9(b) denotes the effect of monomer concentration on the swelling ratio of the NIPA/M-NCC nanocomposite hydrogel at room temperature. The swelling ratio increases as the monomer concentration increases from 2 to 4 M. This is attributed to increased hydrophilic poly (NIPA) chains with low network inhomogeneities due to the relatively lesser M-NCC.

Conclusion

In summary, we have developed a novel approach to prepare vinyl groups incorporated biofriendly M-NCC crosslinker that enables covalent crosslinking during free radical polymerization, eliminating the need to use conventional crosslinkers. The synthesized M-NCC crosslinker has demonstrated an excellent ability to establish covalent and non-covalent connections with polymer chains. Incorporating the M-NCC crosslinker into the poly (NIPA) matrix has resulted in hydrogels with exceptional flexibility, mechanical strength, and swelling capacity. The presence of M-NCC crosslinker has significantly improved the mechanical performance of the hydrogel, enhancing its tensile and compressive strength, toughness, elongation at break, Young's module, and so on. This approach offers a safer alternative to toxic conventional crosslinkers in polymerization reactions. In contrast to polymers formed using conventional crosslinkers, which often exhibit rapid breakage under applied stress due to their covalently crosslinked short polymer chains, the hydrogels prepared with M-NCC crosslinker possess remarkable tensile extensibility, making them highly suitable for biomedical applications. The unique combination of physical and chemical crosslinking sites in the M-NCC crosslinker as well as the uniform dispersibility of M-NCC contribute to the extraordinary mechanical strength of the hydrogels. Furthermore, the interactions between the crosslinker and polymer chains are suitable for uniform energy dissipation under applied stress within the hydrogel matrix, thereby limiting crack propagation.

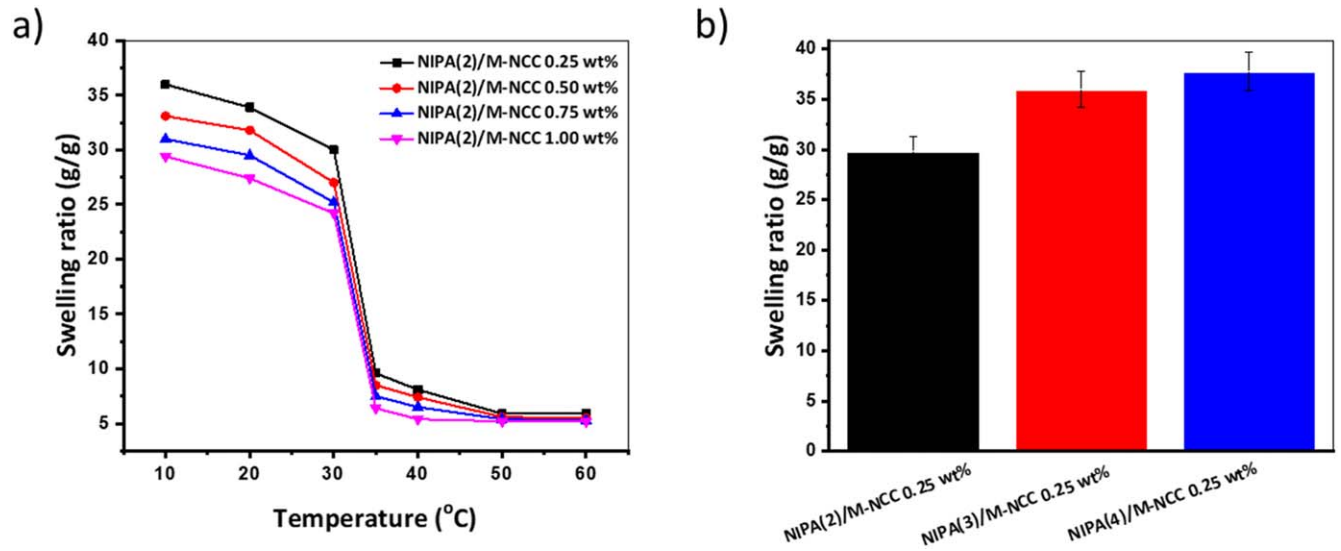

Figure 9. (a) Temperature-dependent swelling behavior of the NIPA(2)/M-NCC nanocomposite hydrogel with varying M-NCC concentrations and (b) swelling behavior of the NIPA/M-NCC nanocomposite hydrogel at room temperature with varying monomer concentrations.

Incorporating M-NCC crosslinking bonds has increased the mechanical properties of the hydrogel while maintaining a temperature-dependent high swelling ratio. The synthesized M-NCC has the potential to serve as a versatile platform for crosslinking various vinyl group polymers, resulting in hydrogels or elastomers with superior mechanical performance. This method opens up possibilities for advanced applications of hydrogels in energy, water treatment, biomedical, and materials engineering fields.

Acknowledgments

A B Imran gratefully acknowledges the support of Capacity Utilization Programme under Special Allocation for Science and Technology from the Ministry of Science and Technology, Peoples Republic of Bangladesh. A B Imran is also thankful to the Committee for Advanced Studies and Research (CASR) in BUET for funding. KSBN is thankful to Durban University of Technology for research fellowship and Director, IWWT, Durban University of Technology.

Data availability statement

All data that support the findings of this study are included within the article (and any supplementary files).

Funding

The authors declare that no funds, grants, or other support were received during the preparation of this manuscript.'

Competing interests

The authors have no relevant financial or non-financial interests to disclose.

ORCID iDs

Suresh Babu Naidu Krishna https://orcid.org/0000-0003-3155-8878
Abu Bin Imran https://orcid.org/0000-0001-8920-8921

References

[1] Imran A B, Seki T and Takeoka Y 2010 Recent advances in hydrogels in terms of fast stimuli responsiveness and superior mechanical performance *Polym. J.* **42** 839–51
[2] Imran A 2020 Design, development, characterization and application of smart polymeric hydrogel *Manufacturing Systems: Recent Progress Future Directions* ed M A Mellal (Nova Science Publishers, Inc.) 1, pp 187–218
[3] Gotoh H, Liu C, Imran A B, Hara M, Seki T and Mayumi K 2018 Optically transparent , high-toughness elastomer using a polyrotaxane cross-linker as a molecular pulley (October) 10.1126/sciadv.aat7629
[4] Ranganathan N, Joseph Bensingh R, Abdul Kader M and Nayak S K 2018 1–25 Synthesis and Properties of Hydrogels Prepared by Various Polymerization Reaction Systems
[5] Shi X, Xu S, Lin J, Feng S and Wang J 2009 Synthesis of SiO_2-polyacrylic acid hybrid hydrogel with high mechanical properties and salt tolerance using sodium silicate precursor through sol-gel process *Mater. Lett.* **63** 527–9
[6] Maitra J and Shukla V K 2014 Cross-linking in hydrogels—a review *Am. J. Polymer Sci.* **4** 25–31
[7] Rangel-Vázquez N A and Leal-García T 2010 Spectroscopy analysis of chemical modification of cellulose fibers *J. Mex. Chem. Soc.* **54** 192–7

[8] Yang W, Zhu L and Chen Y 2015 One-step fabrication of 3-methacryloxypropyltrimethoxysilane modified silica and investigation of fluorinated polyacrylate/silica nanocomposite films *RSC Adv.* **5** 58973–9

[9] Ihsan A B, Imran A B and Susan M A B H 2023 Advanced functional polymers: properties and supramolecular phenomena in hydrogels and polyrotaxane-based materials *Chem. Africa* **6** 79–94

[10] Karim M R, Harun-Ur-Rashid M and Imran A B 2023 Effect of sizes of vinyl modified narrow-dispersed silica cross-linker on the mechanical properties of acrylamide based hydrogel *Sci. Rep.* **13** 5089

[11] Rezaul Karim M, Harun-Ur-Rashid M and Imran A B 2020 Highly stretchable hydrogel using vinyl modified narrow dispersed silica particles as cross-linker *ChemistrySelect* **5** 10556–61

[12] Lee K Y and Mooney D J 2001 Hydrogels for tissue engineering *Chem Rev.* **101** 1869–79

[13] Feng J, Ton X A, Zhao S, Paez J I and del Campo A 2017 Mechanically reinforced catechol-containing hydrogels with improved tissue gluing performance *Biomimetics* **2** 1–15

[14] Schmidt D, Shah D and Giannelis E P 2002 New advances in polymer/layered silicate nanocomposites *Curr. Opin. Solid State Mater. Sci.* **6** 205–12

[15] Gupta P, Vermani K and Garg S 2002 Hydrogels: from controlled release to pH-responsive drug delivery *In: Drug Discovery Today* **7** 569–79

[16] Lin C C and Metters A T 2006 Hydrogels in controlled release formulations: network design and mathematical modeling *Adv. Drug. Del. Rev.* **58** 1379–408

[17] Fu L H, Qi C, Ma M G and Wan P 2019 Multifunctional cellulose-based hydrogels for biomedical applications *J. Mater. Chem.* B **7** 1541–62

[18] Imran D 2019 Superabsorbent hydrogels from carboxymethyl cellulose, Ist edn *400 Oser Avenue, Suite 1600, Hauppauge, NY 11788-3619* (Nova Science Publishers, Inc.)

[19] Caló E and Khutoryanskiy V V 2015 Biomedical applications of hydrogels: a review of patents and commercial products *Eur. Polym. J.* **65** 252–67

[20] Ahmed E M 2015 Hydrogel: preparation, characterization, and applications: a review *J. Adv. Res.* **6** 105–21

[21] Liu L, Li L, Qing Y, Yan N, Wu Y, Li X and Tian C 2016 Mechanically strong and thermosensitive hydrogels reinforced with cellulose nanofibrils *Polym. Chem.* **7** 7142–51

[22] Tan M, Wang J, Song W, Fang J and Zhang X 2019 Self-floating hybrid hydrogels assembled with conducting polymer hollow spheres and silica aerogel microparticles for solar steam generation *J. Mater. Chem.* A **7** 1244–51

[23] Coronado R, Pekerar S, Lorenzo A T and Sabino M A 2011 Characterization of thermo-sensitive hydrogels based on poly(N-isopropylacrylamide)/hyaluronic acid *Polym. Bull.* **67** 101–24

[24] Peng N, Wang Y, Ye Q, Liang L, An Y, Li Q and Chang C 2016 Biocompatible cellulose-based superabsorbent hydrogels with antimicrobial activity *Carbohydr. Polym.* **137** 59–64

[25] Fan H, Wang J and Jin Z 2018 Tough, swelling-resistant, self-healing, and adhesive dual-cross-linked hydrogels based on polymer-tannic acid multiple hydrogen bonds *Macromolecules* **51** 1696–705

[26] Kowalski G, Kijowska K, Witczak M, Kuterasiński L and Lukasiewicz M 2019 Synthesis and effect of structure on swelling properties of hydrogels based on high methylated pectin and acrylic polymers *Polymers* **11** 1–16

[27] Huang T, Xu H, Jiao K, Zhu L, Brown H R and Wang H 2007 A novel hydrogel with high mechanical strength: a macromolecular microsphere composite hydrogel *Adv. Mater.* **19** 1622–6

[28] Han J and Zhang Z 2018 High efficiently numerical simulation of the TDGL equation with reticular free energy in hydrogel *Numerical Analysis* **1** 1–17

[29] Mailly D, Chappert C, Mathet V, Warin P, Chapman J N, Magn T, Jian B, Gong P and Katsuyama Y 2003 Double-network hydrogels with extremely high mechanical strength **14** 2001–4

[30] Imran A B, Esaki K, Gotoh H, Seki T, Ito K, Sakai Y and Takeoka Y 2014 Extremely stretchable thermosensitive hydrogels by introducing slide-ring polyrotaxane cross-linkers and ionic groups into the polymer network *Nat. Commun.* **5** 1–8

[31] Imran A B, Seki T, Ito K and Takeoka Y 2010 Facile synthesis of sliding poly (NIPA) gels using a vinyl modified polyrotaxane as a cross-linker *Trans. Mater. Res. Soc. Jpn* **35** 841–4

[32] Imran A B, Seki T, Ito K and Takeoka Y 2010 Hydrophobic and hydrophilic polyrotaxane based movable cross-linkers for thermo-sensitive poly (N-isopropylacrylamide) gels *Trans. Mater. Res. Soc. Jpn* **35** 291–7

[33] Haraguchi K and Takehisa T 2002 Nanocomposite hydrogels: a unique organic-inorganic network structure with extraordinary mechanical, optical, and swelling/De-swelling properties *Adv. Mater.* **14** 1120–4

[34] Chowdhury A-N, Shapter J and Imran A B 2015 *Innovations in Nanomaterials* (Nova Publishers)

[35] Lee E *et al* 2019 High-performance acellular tissue scaffold combined with hydrogel polymers for regenerative medicine *ACS Biomater. Sci. Eng.* **5** 3462–74

[36] Ngandeu Neubi G M, Opoku-Damoah Y, Gu X, Han Y, Zhou J and Ding Y 2018 Bio-inspired drug delivery systems: An emerging platform for targeted cancer therapy *Biomater. Scie.* **6** 958–73 Royal Society of Chemistry

[37] Lanzalaco S and Armelin E 2017 Poly(N-isopropylacrylamide) and copolymers: a review on recent progresses in biomedical applications *Gels* **3** 36–36

[38] Lu D R, Xiao C M and Xu S J 2009 Starch-based completely biodegradable polymer materials *Express Polymer Lett.* **3** 366–75

[39] Doppalapudi S, Katiyar S and Domb A J 2015 Biodegradable Natural Polymers *Advanced Polymers in Medicine* ed P Francesco (Switzerland: Springer International) 33–66

[40] Athukoralalage S S, Balu R, Dutta N K and Choudhury N R 2019 3D bioprinted nanocellulose-based hydrogels for tissue engineering applications: a brief review *Polymers* **11** 1–13

[41] Pandey J K, Takagi H, Nakagaito A N and Kim H J 2015 *Handbook of Polymer Nanocomposites. Processing, Performance and Application* (Switzerland AG: Springer Nature) Volume C: Polymer nanocomposites of cellulose nanoparticles (https://doi.org/10.1007/978-3-642-45232-1)

[42] Bortolin A, Aouada F A, Mattoso L H C and Ribeiro C 2013 Nanocomposite PAAm/methyl cellulose/montmorillonite hydrogel: Evidence of synergistic effects for the slow release of fertilizers *J. Agric. Food Chem.* **61** 7431–9

[43] Palantöken S, Bethke K, Zivanovic V, Kalinka G, Kneipp J and Rademann K 2020 Cellulose hydrogels physically crosslinked by glycine: synthesis, characterization, thermal and mechanical properties *J. Appl. Polym. Sci.* **137** 23–5

[44] Hossain M A, Roy C K, Sarkar S D, Roy H, Howlader A H and Firoz S H 2020 Improvement of the strength of poly(acrylic acid) hydrogels by the incorporation of functionally modified nanocrystalline cellulose *Mater. Adv.* **1** 2107–16

[45] Du H, Liu W, Zhang M, Si C, Zhang X and Li B 2019 Cellulose nanocrystals and cellulose nanofibrils based hydrogels for biomedical applications *Carbohydr. Polym.* **209** 130–44

[46] Yang J, Han C R, Xu F and Sun R C 2014 Simple approach to reinforce hydrogels with cellulose nanocrystals *Nanoscale* **6** 5934–43

[47] Chau M, France K J D, Kopera B, Machado V R, Rosenfeldt S, Chan K J W, Förster S, Cranston E D, Hoare T and Kumacheva E 2016 Composite hydrogels with tunable anisotropic morphologies and mechanical properties *Chem. Mater.* **28** 3406–15

[48] Liu Y J, Cao W T, Ma M G and Wan P 2017 Ultrasensitive wearable soft strain sensors of conductive, self-healing, and elastic hydrogels with synergistic 'soft and hard' hybrid networks *ACS Appl. Mater. Interfaces* **9** 25559–70

[49] Abdollahi Z, Zare E N, Salimi F and Tay F R 2021 Bioactive carboxymethyl starch-based hydrogels decorated with cuo nanoparticles: antioxidant and antimicrobial properties and accelerated wound healing *in vivo International Journal of Molecular Sciences* **22** 2531

[50] Ounkaew A, Kasemsiri P, Jetsrisuparb K, Uyama H and Hsu Y-I 2020 Synthesis of nanocomposite hydrogel based carboxymethyl starch/polyvinyl alcohol/nanosilver for biomedical materials *Carbohydr Polym* **248** 116767

[51] Pereira K A B, Aguiar K L N P, Oliveira P F, Vicente B M, Pedroni L G and Mansur C R E 2020 Synthesis of hydrogel nanocomposites based on partially *ACS Omega* **5** 4759–69

[52] Hizukuri S, Takeda Y, Yasuda M and Suzuki A 1981 Multi-branched nature of amylose and the action of debranching enzymes *Carbohydr. Res.* **94** 205–13

[53] Shirgholami M A, Shateri Khalil-Abad M, Khajavi R and Yazdanshenas M E 2011 Fabrication of superhydrophobic polymethylsilsesquioxane nanostructures on cotton textiles by a solution-immersion process *J. Colloid Interface Sci.* **359** 530–5

[54] Shen J, Yan B, Li T, Long Y, Li N and Ye M 2012 Mechanical, thermal and swelling properties of poly(acrylic acid)-graphene oxide composite hydrogels *Soft Matter* **8** 1831–6

[55] Shekhar S, Mukherjee M and Sen A K 2012 Studies on thermal and swelling properties of poly (NIPAM-co-2-HEA) based hydrogels *Adv. Mater. Res.* **1** 269–84

[56] Manek E, Domján A, Menyhárd A and László K 2015 Host-guest interactions in poly(N-isopropylacrylamide) gel: a thermoanalytical approach *J. Therm. Anal. Calorim.* **120** 1273–81

[57] Bauri K, Roy S G, Arora S, Dey R K, Goswami A, Madras G and De P 2013 Thermal degradation kinetics of thermoresponsive poly(N- isopropylacrylamide-co-N,N-dimethylacrylamide) copolymers prepared via RAFT polymerization *J. Therm. Anal. Calorim.* **111** 753–61

[58] Zhang J, Hou S, Chen Y, Zhou J, Chen H and Tan Y 2019 Dual-cross-linked dynamic hydrogels with cucurbit[8]uril and imine linkages *Soft Matter* **15** 9797–804

[59] Lee W F and Chen Y J 2001 Studies on preparation and swelling properties of the N-isopropylacrylamide/chitosan semi-IPN and IPN hydrogels *J. Appl. Polym. Sci.* **82** 2487–96